

The effect of heaving motion of multiple wave energy converters installed on a floating platform on global performance

Dongeun Kim^{1a}, Yeonbin Lee^{2b} and Yoon Hyeok Bae^{*3}

¹Multidisciplinary Graduate School Program for Wind Energy, Jeju National University,
102 Jejudaehak-ro, Jeju-si, Jeju-do, 63243, Republic of Korea

²Department of Mechanical Engineering, Hongik University,
94, Wausan-ro, Mapo-gu, Seoul, 04066, Republic of Korea

³Department of Mechanical & System Design Engineering, Hongik University,
94, Wausan-ro, Mapo-gu, Seoul, 04066, Republic of Korea

(Received November 15, 2023, Revised December 19, 2023, Accepted December 20, 2023)

Abstract. Targeting a floating wave and offshore wind hybrid power generation system (FWWHybrid) designed in the Republic of Korea, this study examines the impact of the interaction, with multiple wave energy converters (WECs) placed on the platform, on platform motion. To investigate how the motion of WECs affects the behavior of the FWWHybrid platform, it was numerically compared with a scenario involving a 'single-body' system, where multiple WECs are constrained to the platform. In the case of FWWHybrid, because the platform and multiple WECs move in response to waves simultaneously as a 'multi-body' system, hydrodynamic interactions between these entities come into play. Additionally, the power take-off (PTO) mechanism between the platform and individual WECs is introduced for power production. First, the hydrostatic/dynamic coefficients required for numerical analysis were calculated in the frequency domain and then used in the time domain analysis. These simulations are performed using the extended HARP/CHARM3D code developed from previous studies. By conducting regular wave simulations, the response amplitude operator (RAO) for the platform of both single-body and multi-body scenarios was derived and subsequently compared. Next, to ascertain the difference in response in the real sea environment, this study also includes an analysis of irregular waves. As the floating body maintains its position through connection to a catenary mooring line, the impact of the slowly varying wave drift load cannot be disregarded. To assess the influence of the 2nd-order wave exciting load, irregular wave simulations were conducted, dividing them into cases where it was not considered and cases where it was included. The analysis of multi-degree-of-freedom behavior confirmed that the action of multiple WECs had a substantial impact on the platform's response.

Keywords: hybrid power generation platform; motion response; multi-degree-of-freedom; numerical analysis; wave energy converter

*Corresponding author, Professor, E-mail: yhae@hongik.ac.kr

^aPh.D. Student, E-mail: d1259@jejunu.ac.kr

^bMaster's Student, E-mail: jjyb0210@g.hongik.ac.kr

1. Introduction

In recent times, power generation using renewable energy sources has been expanding to offshore areas due to spatial and societal constraints onshore (Butterfield *et al.* 2005). Efforts are being made globally through various methods to decrease the Levelized Cost of Energy (LCOE) for it, aiming to compete economically with power generation using fossil fuels. One of them is to increase the power generation efficiency per unit area. In the case of wind energy, research has been conducted on the optimal placement to minimize the wake effect of wind turbines or the installation costs (Marmidis *et al.* 2008, Barthelmie *et al.* 2009, Emami and Noghreh 2010, Sarker and Faiz 2017). In the wave energy sector, research on the hydrodynamic effects caused by the arrangement of wave energy converters (WECs) has been investigated, with a focus on employing these findings to improve power generation performance (Taghipour and Moan 2008, Kim and Bae 2019, Kim *et al.* 2020, Poguluri *et al.* 2021). Another method, not involving optimal placement, is a hybrid generation system that simultaneously generates power from two or more renewable energy sources. Among them, wind energy and wave energy generally exhibit a correlation in occurrence (Hanley *et al.* 2010, Chiapponi *et al.* 2020). Applying this, it is possible to devise a system that combines the energy of wind and waves, and research on various floating wave and offshore wind hybrid power generation systems (FWWHybrid) has already been carried out, particularly in Europe (Perez-Collazo *et al.* 2015). Denmark's Poseidon (Floating Power Plant A/S 2015, Yde *et al.* 2015), the UK's Wave Treader (Green Ocean Energy 2015), and Norway's W2-Power (Pelagic Power 2015, Hanssen *et al.* 2015, Legaz *et al.* 2018) are representative examples of marine structures in the form of hybrid power generation. In addition to these, numerous studies have been conducted on various FWWHybrid models (Soulard *et al.* 2013, Muliawan *et al.* 2013, Hallak *et al.* 2018, Kamarlouei *et al.* 2020, Ghafari *et al.* 2021, Yazdi *et al.* 2023, Zhou *et al.* 2023).

The concept and basic design of Korean FWWHybrid (K-FWWHybrid) have been progressively developed in the Republic of Korea since 2013 (Kim *et al.* 2015, Park *et al.* 2015, Kim *et al.* 2016, Song *et al.* 2016, Bae and Lee 2016, Lee *et al.* 2016, Lee *et al.* 2018a, b, Jang *et al.* 2019). K-FWWHybrid is based on a square-shaped semisubmersible platform, as shown in Figs. 1(a) and 1(b). On the upper part, four wind turbines are installed, and a total of 24 cylindrical WECs are arranged, with six on each side. Each WEC is linked to the platform through a linear generator, extracting electrical energy by undergoing vertical motion (heave) along with the waves. Degrees-of-freedom, aside from heave, are constrained to the platform and behave together. Furthermore, the platform is connected with a total of 8 mooring lines—2 attached to each column—to minimize drift, and stability is maintained by affixing damping plates, as shown in Fig. 1(b).

When multiple floating bodies are arranged to move simultaneously, hydrodynamic interactions occur due to radiation and diffraction between these objects (McIver 1984, Mavrakos 1991). Additionally, the platform and each WEC extract electric power of the power generation system by converting mechanical energy to electric energy through a linear generator. In this case, multiple WECs absorb wave energy and act as dampers on the platform motion due to the Power Take-Off (PTO) mechanism from the linear generator (Karimirad 2014). Furthermore, K-FWWHybrid obtains restoring forces for horizontal motion from mooring lines, resulting in a long natural period. 2nd-order slow drift motions also occur in heave, roll, and pitch as the platform freely floats with a low waterplane area (Faltinsen 1993). In this study, motion equations in the time domain were formulated to consider the phenomena mentioned above. For a comparative analysis according to the effect of WEC behavior, numerical simulations were carried out, distinguishing scenarios as shown in Fig. 2:

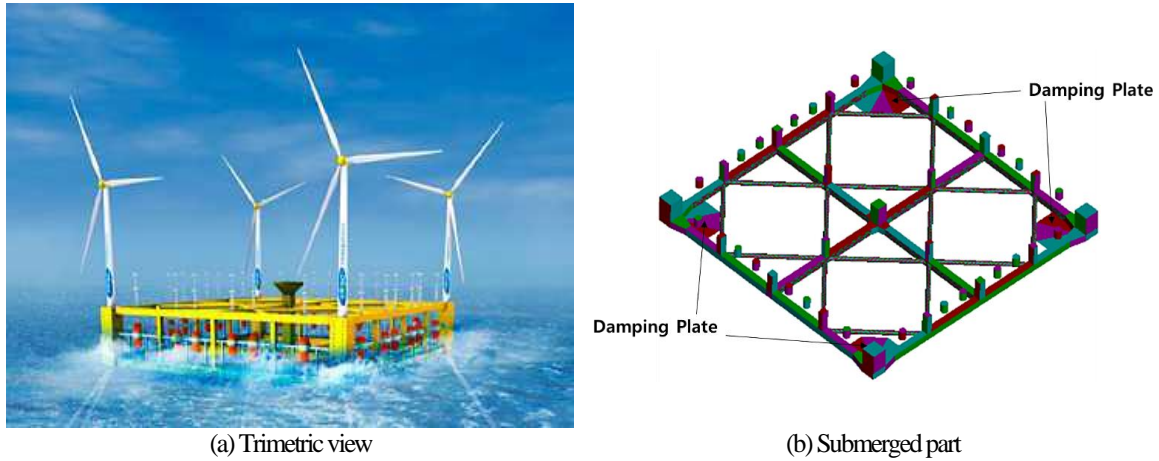


Fig. 1 Conceptual design of Korean floating wave and offshore wind hybrid power generation system

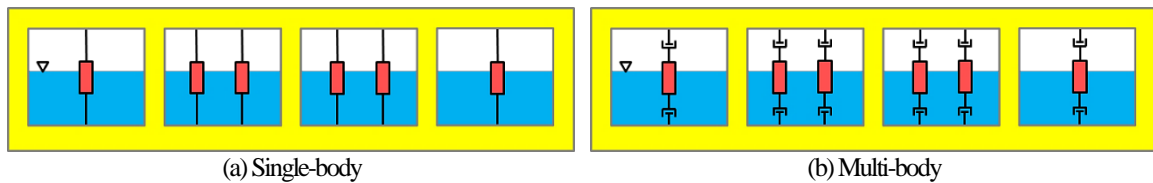


Fig. 2 Configuration of simulation scenarios

one where the floating platform and multiple WECs were assumed as a single rigid body (single-body), and the other where the WECs independently undergo heaving motion within the platform (multi-body). Finally, the study investigated the impact of the heaving motion of multiple WECs placed on a floating platform on the platform's response.

2. Numerical analysis

2.1 Configuration of numerical analysis

The specifications of the K-FWWHybrid, the subject of this study, are summarized in Table 1. On the upper part of the platform, wind turbines operate to generate electricity. However, since the primary objective of this study is to investigate alterations in the platform's behavior due to the motion of multiple WECs with the waves, the operation of the wind turbines is omitted. Instead, the platform and 4 wind turbines are modeled collectively as a single rigid body. The undamped natural periods $T_{N,i}$ for the platform and a single WEC in Table 1 were calculated using Eq. (1), assuming that each individual object behaves as a one degree-of-freedom mass-spring system.

$$T_{N,i} = 2\pi \sqrt{\frac{m_{ij} + a_{ij}}{k_{ij}}} \quad (1)$$

Table 1 Specifications of the platform, single wave energy converter, and mooring line

Property	Unit	Value
Platform without multiple WECs		
Mass, including 4 wind turbines	ton	25,146
Draft	m	15
Width	m	150
Vertical position of CoG* w.r.t SWL**	m	-0.66
Undamped natural period, $T_{N,i}$ (heave / roll / pitch)	s	25.3 / 25.0 / 25.0
Wave energy converter		
Mass	ton	74
Draft	m	5.0
Radius	m	2.0
Vertical position of CoG w.r.t SWL	m	1.91
Undamped natural period, $T_{N,i}$ (heave)	s	5.46
Mooring line		
Number of mooring lines	EA	8
Mooring line type	-	Chain
Water depth	m	80.0
Depth to fairlead below SWL	m	13.0
Depth to anchor below SWL	m	80.0
Mass density (dry weight)	kg/m	432.0
Axial stiffness	kN	1,845,000
Unstretched mooring line length	m	500.0
Mass of clump weight in water	kg	11,000
Number of clump weights per line	EA	6

* CoG : Center of gravity

** SWL : Still water level

The subscripts i and j represent the degrees-of-freedom of the floating bodies, and when calculating $T_{N,i}$, the values for the case where $i = j$ are used. The terms m_{ij} , a_{ij} , and k_{ij} represent the mass (or moment of inertia) and coefficients of added mass (or added moment of inertia) and hydrostatic load (force and moment), respectively. These coefficients are computed from the three-dimensional diffraction/radiation analysis program WAMIT (Wave Analysis MIT), based on linear potential flow theory.

The 24 WECs are linked to the platform via linear generators. However, as they exhibit independent heaving motion, a multi-body dynamic analysis is required. In such a scenario, it is crucial to incorporate the hydrodynamic interaction and the effects of the PTO mechanism between multiple WECs and the platform. Consequently, the motion equations for both the multiple WECs and the platform cannot be expressed independently; they should be established as a system of coupled equations to account for both hydrodynamic and mechanical interactions. In addition, the moored platform has a long natural period. In this case, it is necessary to consider 2nd-order wave exciting loads, such as slowly varying wave drift loads. Despite their small magnitudes, these loads

play a significant role in observing resonances in the low-frequency range. In this study, we developed the multi-degree-of-freedom coupled equation of motion in the time domain proposed by Bae and Lee (2017) to apply various nonlinear external loads. As a comparative reference, numerical simulations were conducted for a single-body scenario where multiple WECs were fixed to the platform to restrict their motion.

2.2 Multi-degree-of-freedom coupled equation of motion in the time domain

By assuming the behavior of floating bodies as a linear system, the frequency domain analysis is relatively straightforward and enables quicker computing. However, for a more accurate realization of motion in real ocean environments, it is advisable to consider time-domain analysis, which can account for various nonlinear external forces. In this study, a multi-degree-of-freedom coupled equation with a total of 30 degrees-of-freedom was developed. The total includes six degrees-of-freedom for the platform and an additional 24 degrees-of-freedom for the 24 WECs undergoing individual heaving motion within the platform. The equation was derived based on the Cummins equation (Cummins 1962). Additionally, the analysis considered the following nonlinear external loads acting on the floating bodies (as depicted in Eq. (2)): damping effect due to fluid viscosity, restoring forces induced by the mooring lines, and 2nd-order wave exciting loads.

$$(M + A)\ddot{\xi}(t) + \int_0^\infty B(\tau)\dot{\xi}(t - \tau)d\tau + L_D(t, \dot{\xi}_{rel}) + B^{PTO}\dot{\xi}(t) + K\xi(t) + L_m(t, \xi) = L_X^{(1)}(t) + L_X^{(2)}(t) \quad (2)$$

In Eq. (2), all terms take the form of a (30x30) matrix or (30x1) vector, taking into account the 30 degrees-of-freedom to reflect the impact of interaction. $\ddot{\xi}$, $\dot{\xi}$, and ξ include the components for acceleration (or angular acceleration), velocity (or angular velocity), and displacement (or angular displacement) of both the platform and WECs, respectively. M denotes the mass (or moment of inertia), and A signifies the added mass (or added mass moment of inertia) as incident wave frequency ω approaches infinity. B(τ) is the retardation function, as shown in Eq. (3).

$$B_{ij}(\tau) = \frac{2}{\pi} \int_0^\infty b_{ij}^{rad}(\omega) \cos(\omega\tau) d\omega \quad (3)$$

K and $L_X^{(1)}(t)$ denote the matrix for the static restoring load coefficients and the vector for the 1st-order wave exciting loads, respectively, both acting on floating bodies. Here, the coefficients for the hydrostatic load, hydrodynamic load (including added mass and radiation damping), and 1st-order wave exciting load applied to Eqs. (2) and (3) were acquired through WAMIT. If a floating body shows symmetry about the X or Y-axis, it is practical to use geometric symmetry when calculating hydrodynamic coefficients. In this study, the geometric shapes of both the platform and WEC exhibit symmetry about the X and Y-axes, leading to the application of symmetry options for each object. Although symmetry options were utilized for individual objects in multi-body simulations, no symmetry option was applied to their arrangement. Each position was independently considered to calculate the hydrodynamic coefficients.

$L_D(t, \dot{\xi}_{rel})$ is the nonlinear viscous drag load, representing the damping effect due to fluid viscosity. It is implemented using Morison drag equation (Morison *et al.* 1950), utilizing the relative velocities ($\dot{\xi}_{rel}$) between the fluid and the floater. $L_m(t, \xi)$ represents the restoring load induced by the mooring line. In this load, the mooring line reaction load against the floater motion is applied by considering the mooring dynamics, including the inertia and drag of each line element based on the finite element method. B^{PTO} denotes the matrix for the PTO damping coefficient. The system

produces electrical power through the relative heave velocity between the platform and each WEC. This relative heave velocity is not only caused by the heave but also by the roll and pitch of the platform. The interaction components of the PTO damping matrix should be configured appropriately to account for these influences. Cho and Choi (2014) conducted a study to calculate the optimal PTO damping coefficient associated with this model. In this analysis, a value of 12,090 kg/s was employed. Power production is described through the PTO mechanism, but the stiffness of the PTO mechanism is not included because it is negligibly small. Instead, PTO damping plays a dominant role in the dynamics. Lastly, $L_X^{(2)}(t)$ represents the 2nd-order wave exciting load. In this study, the slowly varying wave drift load is applied, utilizing difference-frequency components as shown in Eq. (4).

$$L_X^{(2)}(t) = \sum_{k=1}^N \sum_{l=1}^N \text{Re}\{Q_{kl}(\beta_k, \beta_l, \tau_k, \tau_l) a_k \cdot a_l \cdot \exp[i(\omega_k - \omega_l)t + (\phi_k - \phi_l)]\} \quad (4)$$

- N : Number of wave components
- Q_{kl} : Quadratic transfer function (QTF)
- β_k, β_l : Wave direction (=wave heading angle)
- τ_k, τ_l : Wave period
- a_k, a_l : Wave amplitude
- ϕ_k, ϕ_l : Random phase

In Eq. (4), Q_{kl} represents the value of QTF required to convert the square of the wave amplitude into 2nd-order wave loads, and in this study, the QTF was obtained from Newman's approximation (Newman 1974), as illustrated in Eq. (5). These coefficients were obtained by directly integrating the pressure on the body surface using WAMIT (Lee and Newman 1991).

$$Q_{kl} = Q_{lk} = \frac{1}{2}(Q_{kk} + Q_{ll}) \quad (5)$$

The subject of comparison for this study is a single-body, where 24 WECs are fixed to the platform. In this scenario, the equation of motion, based on Eq. (2), is formulated using matrices or vectors with six degrees-of-freedom. Furthermore, since the PTO mechanism is inactive for a single-body case, the term for PTO damping load has been excluded. The HARP/CHARM3D code (Kim *et al.* 2001) was extended and enhanced for numerical simulations, making use of Eq. (2).

3. Numerical analysis results and discussion

3.1 Regular wave simulations

The floating body's motion in the regular wave simulations typically displays a periodic response that follows the incident wave. The essential behavioral characteristics can be discerned by summarizing the floating body's response according to the period of the incident wave. During simulation, it is necessary to gradually increase the wave elevation in a ramped stage to minimize initial transient responses. In regular wave analysis, achieving a steady state in the behavior of the platform involved adding a 600-second stage after a sufficient ramped stage. Utilizing response data from this stage, the Response Amplitude Operator (RAO) for platform motion based on wave frequencies is obtained by calculating the average motion amplitude (ξ^*) and dividing it by the

amplitude of the incident wave (A_{wave}), as shown in Eq. (6).

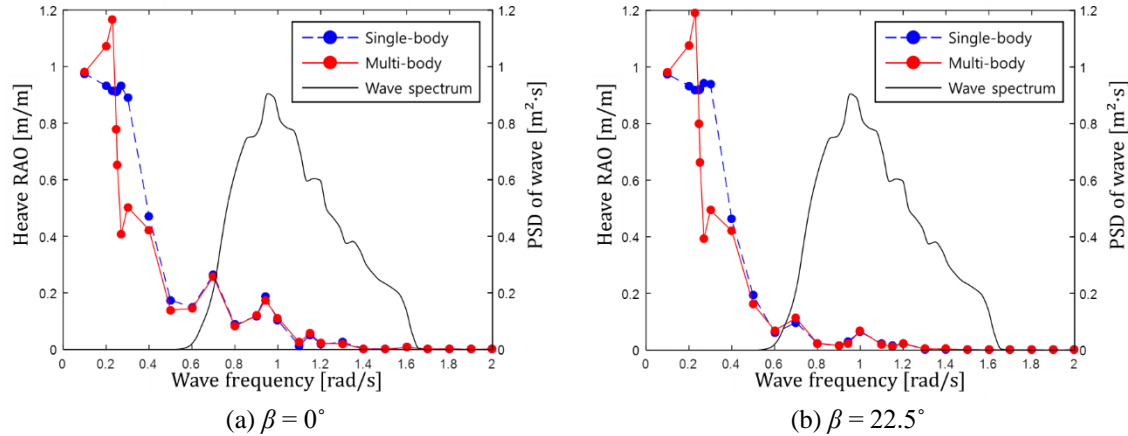


Fig. 3 Heave RAO of the platform in regular waves (wave height = 3.0 m) and power spectral density (PSD) for the incident wave at installation site (JONSWAP Spectrum, $H_s=3.0$ m, $T_p=6.65$ s, $\gamma=1.0$)

Table 2 Environmental conditions

Parameter	Unit	Value
Wave spectrum type		JONSWAP
Water depth	m	80
Significant wave height	m	3
Peak wave period	s	6.67
Peak enhancement factor	-	1.0

$$RAO = \left| \frac{\xi^*}{A_{wave}} \right| \quad (6)$$

In this study, the focus was on generating electrical power by the relative vertical motion between the platform and WEC. As a result, our observations were confined to heave motion. While the platform's roll and pitch also contribute to relative vertical motion, their impact was considered relatively minor compared to heave. In the regular wave simulation, the wave frequencies were initially configured with a 0.1 rad/s interval, ranging from 0.1 rad/s to 2.0 rad/s. To better observe the resonance of the platform, a more refined segmentation was implemented for a specific range (0.2–0.4 rad/s), encompassing the natural frequency of the platform. Furthermore, to assess the influence of the WEC's heave resonance, the natural frequency for the WEC heave (1.15 rad/s) was also considered. Subsequently, the wave height was adjusted to 3m, and the wave heading angle (β) was simulated for two cases: 0° and 22.5° , which are the main wave directions at the platform installation site. Fig. 3 presents the heave RAO results for both the single-body and multi-body scenarios across a total of 26 wave frequencies in the regular wave simulation. Furthermore, a comparison was made with the spectrum of the incident wave at the installation site to anticipate responses in the real sea. The relevant parameters are outlined in Table 2.

Examining Fig. 3(a) with a wave heading angle of 0° , the motion responses of both the single-

body and multi-body are generally similar within the frequency range of the wave spectrum.

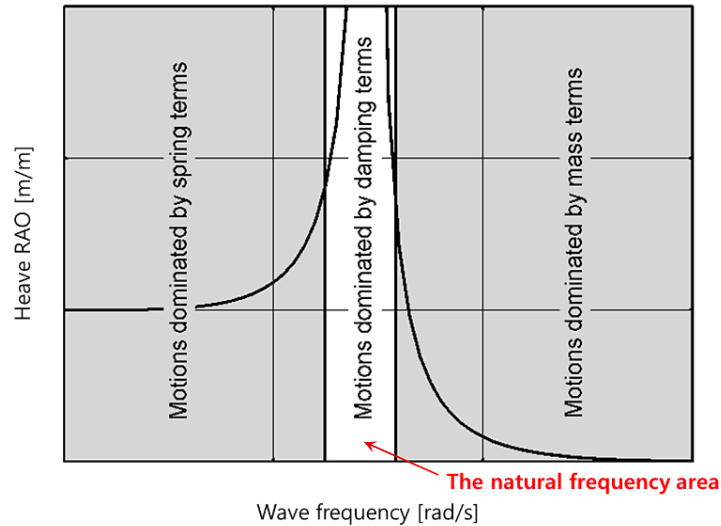


Fig. 4 Frequency areas with respect to motional behavior [Source : *Journee and Massie (2001)*]

However, notable distinctions become evident outside this range, specifically in the range of 0.2–0.4 rad/s. In this regard, the following approach was taken.

The first approach focuses on the phase difference between the platform and the WEC. In both scenarios, where the platform and multiple WECs are present, diffraction due to waves and radiation effects caused by the behavior of the floating body are observed. In the single-body scenario, where multiple WECs are constrained to the platform and move together, they have no choice but to behave in the same phase angle. However, in the multi-body scenario, each WEC and the platform can move independently in heave, phase differences between motions may occur depending on the wave frequency. These phase differences may have either a positive or negative effect on the platform motion. In a simple example, when the phases of the platform and WEC are opposite, the relative vertical motion between them will increase, resulting in an enhanced extraction of power. This suggests that the damping force from the PTO will be greater, leading to a reduction in platform motion. Conversely, when they operate with a smaller phase difference, the impact on motion reduction will be less pronounced. Additionally, the radiation interaction caused by WEC motion will also influence the platform motion, with the extent of influence depending on the phase difference.

The second approach focuses on the significant difference observed in the frequency range, especially around the natural frequency of the platform heave (approximately 0.25 rad/s). According to *Journee and Massie (2001)*, the damping term has a dominant impact on the heave response in the natural frequency region (refer to Fig. 4). In multi-body simulations, the PTO damping effect is considered, while in single-body simulations, it is not applied. Consequently, in multi-body simulations, response changes near the natural frequency are noted to be highly sensitive, contributing to a significant contrast with the response observed in single-body simulations.

Even when the wave heading angle is 22.5° , a similar trend is observed compared to when it is 0° , but the response within the frequency range of the wave spectrum is relatively diminished. Therefore, it can be anticipated that the platform's behavior will decrease in the real sea when β is

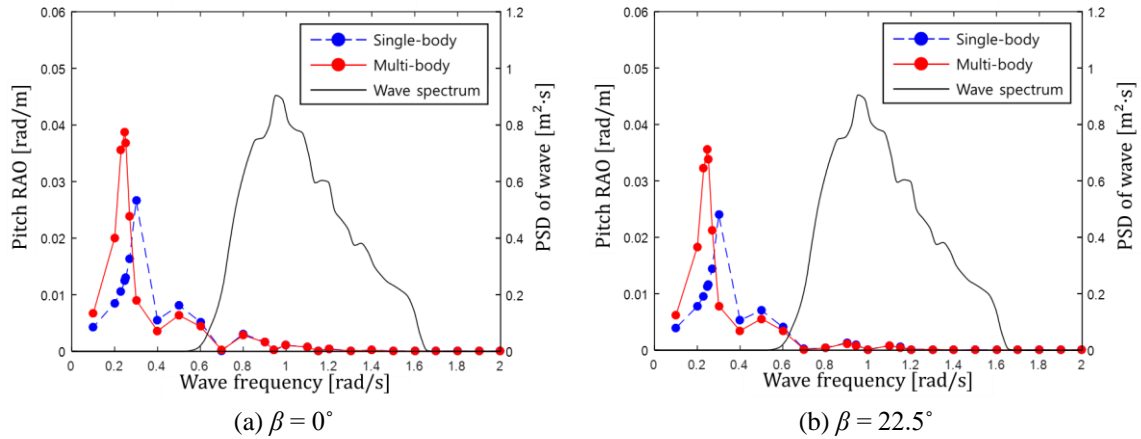


Fig. 5 Pitch RAO of the platform in regular waves (wave height = 3.0 m) and power spectral density (PSD) for the incident wave at installation site (JONSWAP Spectrum, $H_s=3.0$ m, $T_p=6.65$ s, $\gamma=1.0$)

22.5°. To verify this, conducting an irregular wave simulation with the application of environmental loads at the installation site is necessary.

As previously mentioned, the heave, roll and pitch of the platform all affect the relative heave motion of the WEC. For this reason, the heave, roll and pitch of the platform are affected by the damping force of the WEC, resulting in heave-roll-pitch coupled motion of the platform. To confirm the effect of this coupling, the pitch RAO results are shown in Fig. 5. However, the amplitude of the pitch is relatively very small, and the natural frequencies of heave and pitch (near 0.251 rad/s) are almost the same as shown in Table 1. Therefore, it is difficult to directly confirm the combined effect through Fig. 5.

3.2 Irregular wave simulations

To investigate the behavior of the platform in real sea conditions, an irregular wave simulation was conducted. Waves were numerically generated using the environmental conditions from Table 2. To minimize initial transient responses, a sufficient ramped stage was employed, and the analysis was carried out over a duration of 10,800 seconds (3 hours). Moreover, numerical analyses were conducted, distinguishing between scenarios considering only the 1st-order wave exciting load and those considering both the 1st- and 2nd-order wave exciting loads.

3.2.1 Consideration on first-order wave exciting load only

Figs. 6 and 7 illustrate time series data representing the displacement and acceleration of the platform's heave under environmental load with only 1st-order wave exciting loads, respectively. In accordance with Newton's second law, which posits that the sum of all external forces acting on an object is equal to the inertial force (proportional to acceleration), acceleration results were compared for comparative robustness analysis of the systems. Subsequently, to investigate changes in motion characteristics, the rates of change in statistics are summarized in Table 3, where the presented values indicate the increase or decrease rate of the multi-body response relative to the single-body response.

When the values in Table 3 are negative, it indicates that the result of the multi-body are smaller

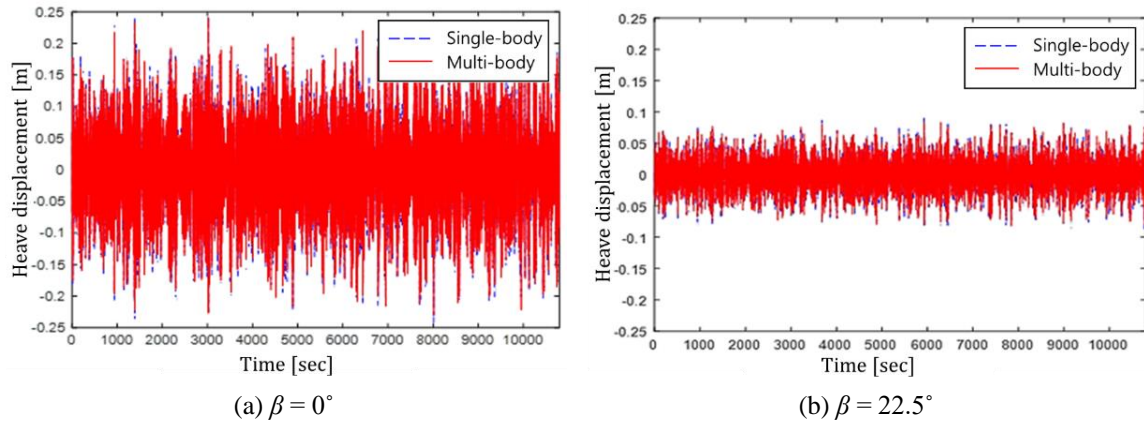


Fig. 6 Time series data for displacement of the platform's heave motion under environmental load, considering only 1st-order wave exciting loads

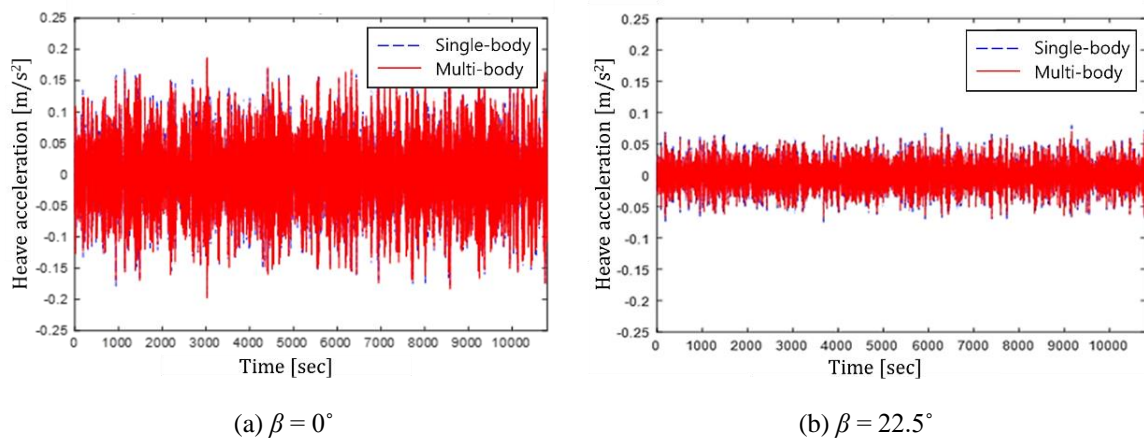


Fig. 7 Time series data for acceleration of the platform's heave motion under environmental load, considering only 1st-order wave exciting loads

than those of the single-body. Given that the majority of displacements and accelerations are negative, it can be inferred that the multi-body exhibits relatively stable behavior. At $\beta = 22.5^\circ$, the peaks of displacement and acceleration decrease by approximately 11.09% and 13.41%, respectively. However, upon reviewing Figs. 6(b) and 7(b), the magnitude of the time series data is small, so the absolute difference between the two datasets may not be significant. To verify this, Fourier transformation was applied, as shown in Figs. 8 and 9, to transform the data into spectra, allowing a comparison of magnitudes based on frequency components in the time history. The comparative results suggest that the outcomes for the two scenarios are nearly identical when β is 22.5° . However, the magnitudes of the spectra between the two scenarios differ slightly when β is 0° . In conclusion, the reduction in platform motion due to the motion of multiple WECs can be explained in the multi-body case compared to the single-body case. Additionally, the smaller response at $\beta = 22.5^\circ$ compared to $\beta = 0^\circ$ aligns with the predictions from the regular wave simulation results.

Table 3 Rate of change in statistics for the platform's heave motion of both scenarios under environmental load, considering only 1st-order wave exciting loads

	[%]	Positive peak	Negative peak	STD*
$\beta = 0^\circ$	Displacement	-1.53	-6.11	-4.05
	Acceleration	-0.69	+0.04	-2.20
$\beta = 22.5^\circ$	Displacement	-10.12	-11.09	-5.12
	Acceleration	-13.41	-8.98	-8.79

*STD : Standard deviation

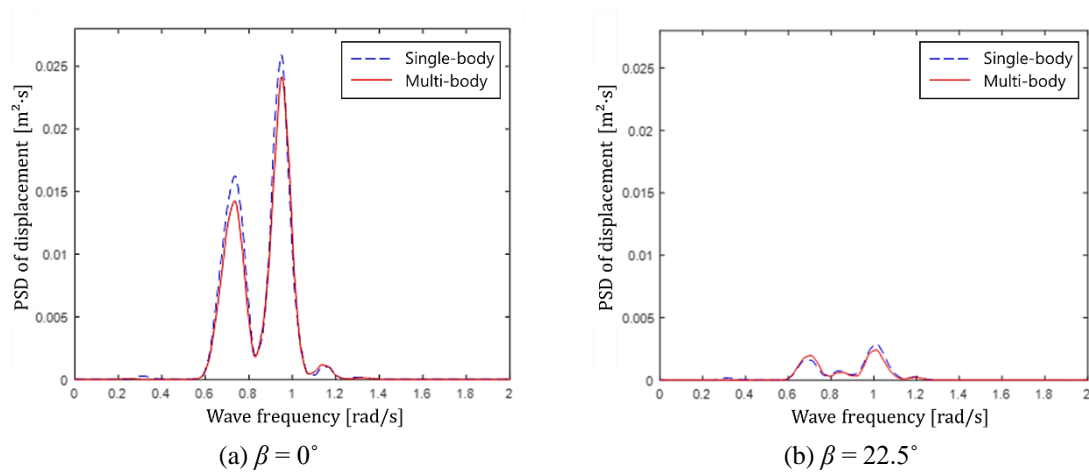


Fig. 8 Power spectral density for displacement of the platform's heave motion under environmental load, considering only 1st-order wave exciting loads

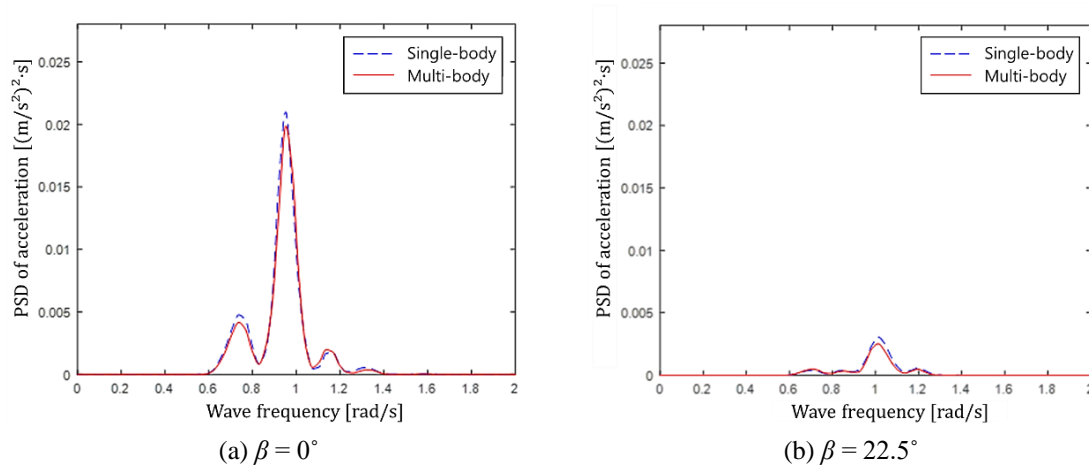


Fig. 9 Power spectral density for acceleration of the platform's heave motion under environmental load, considering only 1st-order wave exciting loads

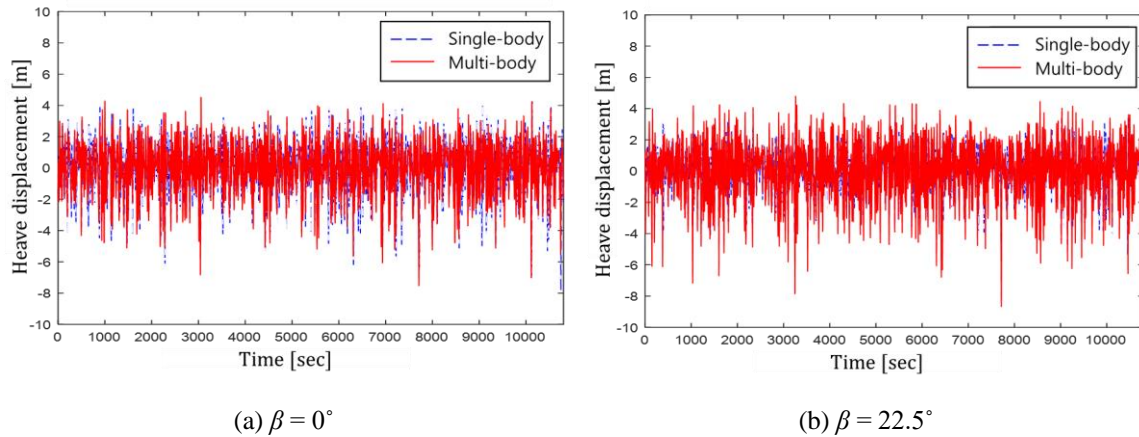


Fig. 10 Time series data for displacement of the platform's heave motion under environmental load, considering both 1st- and 2nd-order wave exciting loads

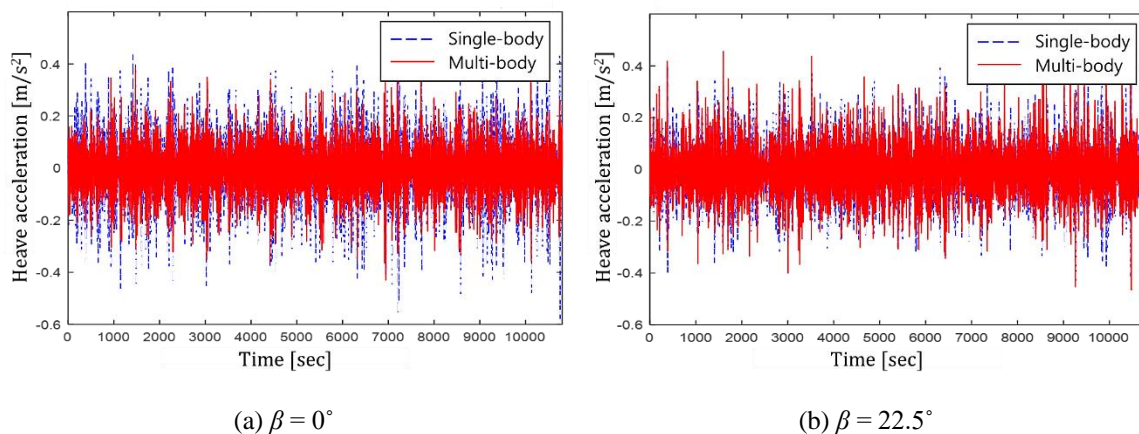


Fig. 11 Time series data for acceleration of the platform's heave motion under environmental load, considering both 1st- and 2nd-order wave exciting loads

3.2.2 Consideration on both first and second-order wave exciting loads

As previously mentioned, the K-FWWHybrid has a low heave natural frequency, requiring consideration of 2nd-order wave exciting loads such as the slowly-varying wave drift force. For this reason, additional irregular wave simulations, accounting for 2nd-order wave exciting loads under the same wave conditions, were conducted. The results are presented in Table 4 and Figs. 10-13.

In comparison, the findings in this section show a different pattern from those in section 3.2.1. Examining Fig. 3, it becomes clear that the peak frequency of the multi-body occurs at a lower frequency than that of the single-body, and the magnitude of the RAO is higher at that frequency. The reason for the lower natural frequency in the multi-body case compared to the single-body case lies in the exclusion of the heave component's mass added to the platform by the 24 WECs. While

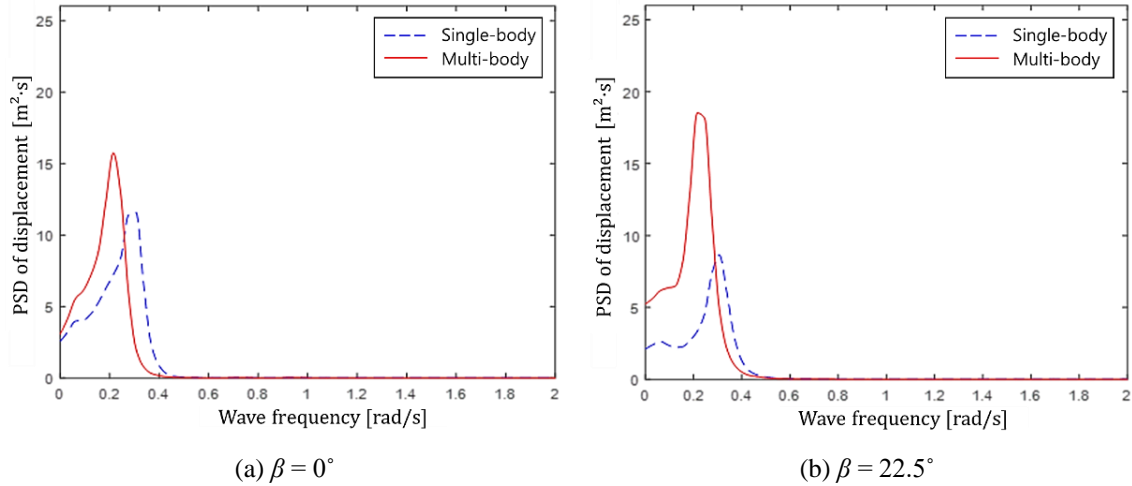


Fig. 12 Power spectral density for displacement of the platform's heave motion under environmental load, considering both 1st- and 2nd-order wave exciting loads

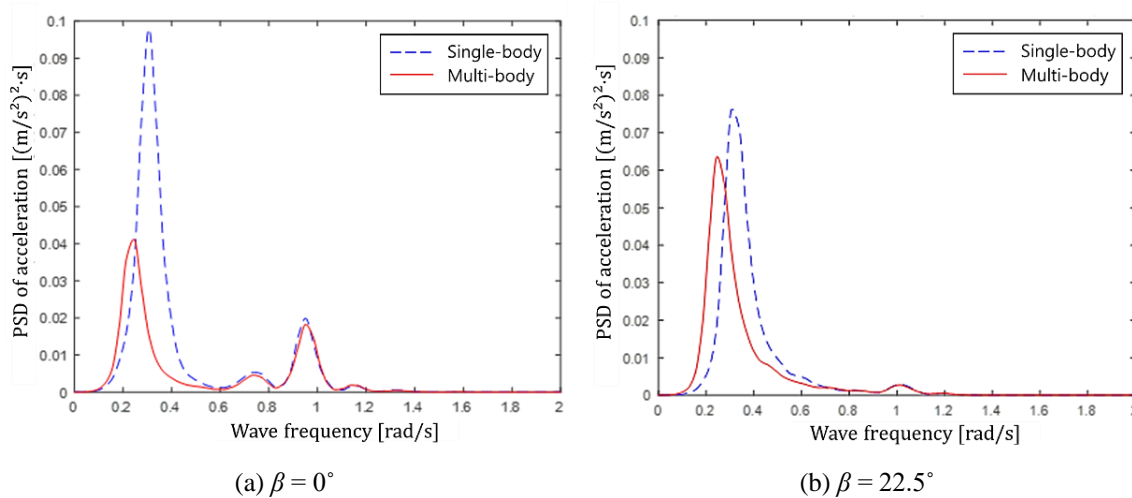


Fig. 13 Power spectral density for acceleration of the platform's heave motion under environmental load, considering both 1st- and 2nd-order wave exciting loads

the additional heave restoring force from the 24 WECs was also excluded, a comprehensive comparison with the single-body case, which includes both the heave mass and restoring force components from the WECs, leads to the judgment that the natural frequency has slightly shifted to a lower frequency. This trend is clearly observed in Fig. 12, where the resonance of the multi-body is more prominently observed due to the consideration of 2nd-order wave exciting loads. Table 4 reveals that when β is 22.5°, the maximum heave of the multi-body is notably 59.28% higher than that of the single-body. However, a comparison of the acceleration spectra at each resonance

Table 4 Rate of change in statistics for the platform's heave motion of both scenarios under environmental load, considering both 1st- and 2nd-order wave exciting loads

	[%]	Positive peak	Negative peak	STD*
$\beta = 0^\circ$	Displacement	+4.40	-4.54	+3.79
	Acceleration	-10.37	-25.77	-26.27
$\beta = 22.5^\circ$	Displacement	+35.63	+59.28	+43.17
	Acceleration	+0.65	+6.7	-6.99

*STD : Standard deviation

frequency indicates different results, with the multi-body exhibiting smaller magnitudes. In essence, the multi-body displays relatively larger displacements, but its advantage in terms of overall system stability comes from the smaller acceleration of motion. This impact is particularly crucial for the performance of the wind turbine mounted on the upper part.

4. Conclusions

In this study, the influence of the degree-of-freedom of 24 WECs installed in a floating wave and offshore wind hybrid power generation system was examined. Two scenarios were investigated: a multi-body case, where the WECs move independently of the platform with their own degrees-of-freedom, and a single-body case, where the WECs are combined with the platform as a single rigid body. The objective is to check and analyze the differences in global performance between these two scenarios. The multiple WECs installed on the platform generate electricity by converting wave energy into electrical energy through a linear generator. Simultaneously, the WECs serve as a damper to reduce the motion of the platform from the PTO mechanism effect. To verify this, multi-degree-of-freedom coupled equation of motion in the time domain, considering the interaction between the six degrees-of-freedom of the platform and the vertical motion of the 24 WECs, was established, and numerical analysis was conducted. Additionally, to confirm the differences in motion, the single-body (compared model) with multiple WECs fixed to a platform was numerically simulated, and its results were compared with the motion responses of the multi-degree-of-freedom system. The incident wave conditions were divided into regular and irregular waves, and numerical analyses were performed for incident wave directions of 0° and 22.5° .

Through the regular waves analysis, the RAOs of the two models (multi-body and single-body) were obtained and compared, but the difference was minimal in the frequency range of the incident wave in real sea conditions. Subsequently, the time series data for displacement and acceleration were calculated through the irregular wave simulation for a duration of 3 hours. The resulting data were then used to calculate statistics and spectra. When considering only the 1st-order wave load, a difference in response occurred between the two cases, but the motion amplitude was too small to be considered significantly meaningful. However, when considering the 2nd-order wave load, the difference between the two cases became evident, particularly as it excited near the natural period of the platform heave. Differences were observed not only in the amplitude of motion but also in the natural frequency of each case due to changes in the mass and restoring force components of the heave in both the single-body and multi-body configurations.

A future study will be essential to investigate how changes in platform motion, induced by multiple wave energy converters, impact the performance of top-mounted wind turbines.

Acknowledgments

This work was supported by 2023 Hongik University Research Fund.

References

- Bae, Y.H. and Lee, H. (2016), "Transient effects of wind-wave hybrid platform in mooring line broken condition", *J. Korean Soc. Mar. Environ. Energy*, **19**(2), 129-136. <https://doi.org/10.7846/JKOSMEE.2016.19.2.129>.
- Bae, Y.H. and Lee, H. (2017), "Multi-DOF time-domain analysis of wind-wave hybrid power generation platform", *J. Korean Soc. Mar. Environ. Energy*, **20**(3), 127-135. <https://doi.org/10.7846/JKOSMEE.2017.20.3.127>.
- Barthelmie, R.J., Hansen, K., Frandsen, S.T., Rathmann, O., Schepers, J.G., Schlez, W., Phillips, J., Rados K., Zervos A., Politis E.S. and Chaviaropoulos P.K. (2009), "Modelling and Measuring Flow and Wind Turbine Wakes in Large Wind Farms Offshore", *Wind Energy: Int. J. Progress Appl. Wind Power Conversion Technol.*, **12**(5), 431-444. <https://doi.org/10.1002/we.348>.
- Butterfield, S., Musial, W., Jonkman, J. and Scavounos, P. (2007), "Engineering challenges for floating offshore wind turbines", National Renewable Energy Lab.(NREL), USA.
- Chiapponi, L., Addona, F., Diaz-Carrasco, P., Losada, M.A. and Longo, S. (2020), "Statistical analysis of the interaction between wind-waves and currents during early wave generation", *Coast. Eng.*, **159**, 103672. <https://doi.org/10.1016/j.coastaleng.2020.103672>.
- Cho, I.H. and Choi, J.Y. (2014), "Design of wave energy extractor with a linear electric generator-part II. linear generator", *J. Korean Soc. Mar. Environ. Energy*, **17**(3), 174-181. <https://doi.org/10.7846/JKOSMEE.2014.17.3.174>.
- Cummins, W.E. (1962), "The impulse response function and ship motions", David Taylor Model Basin Washington DC.
- Emami, A. and Pirooz, A. (2010), "New approach on optimization in placement of wind turbines within wind farm by genetic algorithms", *Renew. Energy*, **35**(7), 1559-1564. <https://doi.org/10.1016/j.renene.2009.11.026>.
- Faltinsen, O. (1993), *Sea Loads on Ships and Offshore Structures*, (1st Ed.), Cambridge university press, Cambridge, UK.
- Floating Power Plant A/S (2015), *Poseidon Floating Power (Poseidon 37)*, Pacific Northwest National Laboratory; WA, USA. <https://tethys.pnnl.gov/project-sites/poseidon-floating-power-poseidon-37>.
- Ghafari, H.R., Ghassemi, H. and Guanghua, H. (2021), "Numerical study of the Wavestar wave energy converter with multi-point-absorber around DeepCwind semisubmersible floating platform", *Ocean Eng.*, **232**, 109177. <https://doi.org/10.1016/j.oceaneng.2021.109177>.
- Green Ocean Energy Wave Treader Project (2010), *The Green Ocean Energy Wave Treader Project*, Power Technology; NY, USA. <https://www.power-technology.com/projects/greenoceanenergywav/>
- Hallak, T.S., Gaspar, J.F., Kamarlouei, M., Calvário, M., Mendes, M.J., Thiebaut, F. and Guedes Soares, C. (2018), "Numerical and experimental analysis of a hybrid wind-wave offshore floating platform's hull", *Proceedings of the International Conference on Offshore Mechanics and Arctic Engineering*, Madrid, Spain, June. <https://doi.org/10.1115/OMAE2018-78744>.
- Hanley, K.E., Belcher, S.E. and Sullivan, P.P. (2010), "A global climatology of wind-wave interaction". *J. Phys. Oceanography*, **40**(6), 1263-1282. <https://doi.org/10.1175/2010JPO4377.1>.

- Hanssen, J.E., Margheritini, L., O'Sullivan, K., Mayorga, P., Martinez, I., Arriaga, A., Agos, I., Steynor, J., Ingram, D., Hezari, R. and Todalsaug, J.H. (2015), "Design and performance validation of a hybrid offshore renewable energy platform", *Proceedings of the 2015 10th International Conference on Ecological Vehicles and Renewable Energies*, Monte Carlo, Monaco, April. <https://doi.org/10.1109/EVER.2015.7113017>.
- Jang, H.K., Park, S., Kim, M.H., Kim, K.H. and Hong, K. (2019), "Effects of heave plates on the global performance of a multi-unit floating offshore wind turbine", *Renew. Energ.*, **134**, 526-537. <https://doi.org/10.1016/j.renene.2018.11.033>.
- Journée, J.M.J. and Massie, W.W. (2001), *Offshore hydromechanics*. Delft University of Technology.
- Kamarlouei, M., Gaspar, J.F., Calvario, M., Hallak, T.S., Mendes, M.J., Thiebaut, F. and Soares, C.G. (2020), "Experimental analysis of wave energy converters concentrically attached on a floating offshore platform", *Renew. Energ.*, **152**, 1171-1185. <https://doi.org/10.1016/j.renene.2020.01.078>.
- Karimirad, M. (2014), *Offshore energy structures: for wind power, wave energy and hybrid marine platforms*, Springer.
- Kim, D. and Bae, Y.H. (2019), "Time domain analysis of optimal arrangement of wave energy converters placed on a floating platform", *J. Korean Soc. Mar. Environ. Energy*, **22**(3), 125-132. <https://doi.org/10.7846/JKOSMEE.2019.22.3.125>.
- Kim, D., Poguluri, S.K. and Bae, Y.H. (2020) "Numerical study on linear behavior of arrayed pitch motion wave energy converter", *J. Korean Soc. Mar. Environ. Energy*, **23**(4), 269-276. <https://doi.org/10.7846/JKOSMEE.2020.23.4.269>.
- Kim, K.H., Lee, K., Sohn, J.M., Park, S., Choi, J.S. and Hong, K. (2015), "Conceptual design of large semi-submersible platform for wave-offshore wind hybrid power generation", *J. Korean Soc. Mar. Environ. Energy*, **18**(3), 223-232. <https://doi.org/10.7846/JKOSMEE.2015.18.3.223>.
- Kim, K.H., Hong, J.P., Park, S., Lee, K. and Hong, K. (2016), "An experimental study on dynamic performance of large floating wave-offshore hybrid power generation platform in extreme conditions", *J. Korean Soc. Mar. Environ. Energy*, **19**(1), 7-17. <https://doi.org/10.7846/JKOSMEE.2016.19.1.7>.
- Kim, M.H., Ran, Z. and Zheng, W. (2001), "Hull/mooring coupled dynamic analysis of a truss spar in time domain", *Int. J. Offshore and Polar Eng.*, **11**(1), 42-54.
- Lee, C.H. and Newman, J.N. (1991) "First- and second-order wave effects on a submerged spheroid", *J. Ship Res.*, **35**(03), 183-190. <https://doi.org/10.5957/jsr.1991.35.3.183>.
- Lee, H., Cho, I.H., Kim, K.H. and Hong, K. (2016), "Interaction analysis on deployment of multiple wave energy converters in a floating hybrid power generation platform", *J. Korean Soc. Mar. Environ. Energy*, **19**(3), 185-193. <https://doi.org/10.7846/JKOSMEE.2016.19.3.185>.
- Lee, H., Bae, Y.H., Kim, D., Park, S., Kim, K.H. and Hong, K. (2018a), "Study on Optimal Damping Model of Very Large Offshore Semi-submersible Structure", *J. Ocean Eng. Technol.*, **32**(1), 1-8. <https://doi.org/10.26748/KSOE.2018.2.32.1.001>.
- Lee, H., Poguluri, S.K. and Bae, Y.H. (2018b), "Performance analysis of multiple wave energy converters placed on a floating platform in the frequency domain", *Energies*, **11**(2), 406. <https://doi.org/10.3390/en11020406>.
- Legaz, M.J., Coronil, D., Mayorga, P. and Fernández, J. (2018), "Study of a hybrid renewable energy platform: W2Power", *Proceedings of the International Conference on Offshore Mechanics and Arctic Engineering*, Madrid, Spain, June. <https://doi.org/10.1115/OMAE2018-77690>.
- Marmidis, G., Lazarou, S. and Pyrgioti, E. (2008), "Optimal placement of wind turbines in a wind park using Monte Carlo simulation", *Renew. Energ.*, **33**(7), 1455-1460. <https://doi.org/10.1016/j.renene.2007.09.004>.
- Mavrikos, S.A. (1991), "Hydrodynamic coefficients for groups of interacting vertical axisymmetric bodies", *Ocean Eng.*, **18**(5), 485-515. [https://doi.org/10.1016/0029-8018\(91\)90027-N](https://doi.org/10.1016/0029-8018(91)90027-N).
- McIver, P. (1984), "Wave forces on arrays of floating bodies", *J. Eng. Mathematics*, **18**(4), 273-285. <https://doi.org/10.1007/BF00042842>.
- Morison, J.R., Johnson, J.W. and Schaaf, S.A. (1950), "The force exerted by surface waves on piles", *J. Petroleum Technol.*, **2**(5), 149-154. <https://doi.org/10.2118/950149-G>.
- Muliawan, M.J., Karimirad, M. and Moan, T. (2013), "Dynamic response and power performance of a

- combined spar-type floating wind turbine and coaxial floating wave energy converter”, *Renew. Energ.*, **50**, 47-57. <https://doi.org/10.1016/j.renene.2012.05.025>.
- Newman, J.N. (1974), “Second-order slowly varying forces on vessels in irregular waves”, In Proceedings of the international symposium on dynamics of marine vehicles and structures in waves. London, UK.
- Park, S., Kim, K.H., Lee, K.S., Park, Y.S., Oh, H., Shin, H. and Hong, K. (2015), “Arrangement design and performance evaluation for multiple wind turbines of 10 MW class floating wave-offshore wind hybrid power generation system”, *J. Korean Soc. Mar. Environ. Energy*, **18**(2), 123-132. <https://doi.org/10.7846/JKOSMEE.2015.18.2.123>.
- Pelagic Power (2015), W2Power, Vanvikan, Norway. <http://www.pelagicpower.no>
- Pérez-Collazo, C., Greaves, D. and Iglesias, G. (2015), “A review of combined wave and offshore wind energy”, *Renew. Sust. Energ. Rev.*, **42**, 141-153. <https://doi.org/10.1016/j.rser.2014.09.032>.
- Poguluri, S.K., Kim, D., Ko, H.S. and Bae, Y.H. (2021), “Performance analysis of multiple wave energy converters due to rotor spacing”, *J. Ocean Eng. Technol.*, **35**(3), 229-237. <https://doi.org/10.26748/KSOE.2021.007>.
- Sarker, B.R. and Faiz, T.I. (2017), “Minimizing transportation and installation costs for turbines in offshore wind farms”, *Renew. Energ.*, **101**, 667-679. <https://doi.org/10.1016/j.renene.2016.09.014>.
- Song, C.Y., Lee, K. and Hong, K. (2016), “Topology optimization application for initial platform design of 10 MW grade floating type wave-wind hybrid power generation system”, *J. Korean Soc. Mar. Environ. Energy*, **19**(3), 194-202. <https://doi.org/10.7846/JKOSMEE.2016.19.3.194>.
- Soulard, T., Babarit, A. and Borgarino, B. (2013), “Preliminary assessment of a semi-submersible floating wind turbine combined with pitching wave energy converters”, *Proceedings of the 10th European Wave and Tidal Energy Conference (EWTEC2013)*, Aalborg, Denmark, September. <https://hal.archives-ouvertes.fr/hal-01201908>
- Taghipour, R. and Moan, T. (2008), “Efficient frequency-domain analysis of dynamic response for the multi-body wave energy converter in multi-directional wave”, *Proceedings of the ISOPE International Ocean and Polar Engineering Conference (pp. ISOPE-I)*, Trondheim, Norway, July.
- Yazdi, H., Ghafari, H.R., Ghassemi, H., He, G. and Karimirad, M. (2023), “Wave power extraction by Multi-Salter's duck WECs arrayed on the floating offshore wind turbine platform”, *Energy*, **278**, 127930. <https://doi.org/10.1016/j.energy.2023.127930>.
- Yde, A., Larsen, T.J., Hansen, A.M., Fernandez, M., Bellew, S. and Plant, F.P. (2015), “Comparison of simulations and offshore measurement data of a combined floating wind and wave energy demonstration platform”, *J. Ocean. Wind Energy*, **2**, 129-137. <https://doi.org/10.17736/jowe.2015.jcr34>.
- Zhou, B., Hu, J., Jin, P., Sun, K., Li, Y. and Ning, D. (2023), “Power performance and motion response of a floating wind platform and multiple heaving wave energy converters hybrid system”, *Energy*, **265**, 126314. <https://doi.org/10.1016/j.energy.2022.126314>.

